Struct Multidisc Optim (2009) 37:239–253
DOI 10.1007/s00158-008-0234-7

REVIEW ARTICLE

A comparative study of uncertainty propagation methods for black-box-type problems

S. H. Lee · W. Chen

Received: 17 June 2007 / Revised: 9 January 2008 / Accepted: 20 January 2008 / Published online: 9 May 2008

Abstract A wide variety of uncertainty propagation methods exist in literature; however, there is a lack of good understanding of their relative merits. In this paper, a comparative study on the performances of several representative uncertainty propagation methods, including a few newly developed methods that have received growing attention, is performed. The full factorial numerical integration, the univariate dimension reduction method, and the polynomial chaos expansion method are implemented and applied to several test problems. They are tested under different settings of the performance nonlinearity, distribution types of input random variables, and the magnitude of input uncertainty. The performances of those methods are compared in moment estimation, tail probability calculation, and the probability density function construction, corresponding to a wide variety of scenarios of design under uncertainty, such as robust design, and reliability-based design optimization. The insights gained are expected to direct designers for choosing the most applicable uncertainty propagation technique in design under uncertainty.

S. H. Lee · W. Chen (✉)
Department of Mechanical Engineering,
Northwestern University, 2145 Sheridan Rd Tech B224,
Evanston, IL 60201, USA
e-mail: weichen@northwestern.edu

S. H. Lee
e-mail: sanghoon-lee@northwestern.edu

Keywords Uncertainty propagation · Full factorial numerical integration · Dimension reduction method · Polynomial chaos expansion · Comparative study · Design under uncertainty

Nomenclature

n	number of input random variables
$\boldsymbol{X}$	vector of input random variables
$f_{\mathbf{X}}(\mathbf{x})$	joint probability density function of $\mathbf{X}$
μ	mean
σ	standard deviation
$\sqrt{\beta_1}$	skewness
β_2	kurtosis
$E[\bullet]$	expectation operator
m	number of nodes (integration points)
$l_{i\cdot j}$	jth node (integration point) of ith random variable
$w_{i\cdot j}$	jth weight of ith random variable
$\hat{y}$	additively decomposed model of y in univariate dimension reduction method
$\xi(\theta)$	standard normal variable with zero mean and unit variance
p	order of PCE
Γ_p	generic element of Hermite polynomial of order p
P	number of terms in PCE
$y^{(P)}$	polynomial chaos expansion of y with P terms
Ψ_i	simplified form of Hermite polynomial $\Gamma_p\left(\xi_{i_1}, \cdots, \xi_{i_n}\right)$
UP	uncertainty propagation
FFNI	full factorial numerical integration
UDR	univariate dimension reduction

PCE polynomial chaos expansion
FORM first-order reliability method
MPP most probable point

1 Introduction

Quantification of uncertainties in system output performances propagated from uncertain inputs, named as the uncertainty propagation (UP), is essential to design under uncertainty. A lot of efforts have been made to develop methods of UP in various fields such as structural reliability (Madsen et al. 2006; Christensen and Baker 1982; Kiureghian 1996), stochastic mechanics (Ghanem and Spanos 1991; Liu et al. 1986), and quality engineering (Evans 1972; Taguchi 1978; D'Errico and Zaino 1988; Seo and Kwak 2002), and a considerable number of methods are now available. Since these methods were developed with different backgrounds and philosophies, it is necessary to examine their applicability and relative merits in the context of engineering design.

In the design under uncertainty, the role that the UP is expected to play varies based on different design scenarios. For instance, in the robust design (Du and Chen 2000; McAllister and Simpson 2003), the interest of UP is to evaluate the low-order moments (mean and variance) of a performance. In the reliability-based design (Lee and Kwak 1987–1988; Wu 1994; Youn et al. 2003; Du et al. 2004), the interest is on assessing the performance reliability. The complete distribution of a performance needs to be assessed in utility optimization (Hazelrigg 1998), where the probability distribution is integrated with the designer's utility function to maximize the expected utility of a product. Our goal in this work is to conduct an in-depth examination of several widely used UP techniques, some being newly developed in literature, to understand the characteristics and limitations of these methods, and to compare their performance using illustrative examples.

The methods for UP can be classified into five categories as follows. The first category is the simulation-based methods like Monte Carlo simulation (MCS; Madsen et al. 2006; Christensen and Baker 1982; Kiureghian 1996), importance sampling (Melchers 1989; Engelund and Rackwitz 1993), and adaptive sampling (Bucher 1988). The second category is the local expansion-based methods like the Taylor series method or perturbation method (Madsen et al. 2006; Christensen and Baker 1982; Kiureghian 1996; Ghanem and Spanos 1991). Methods in this category are weak against the large variability of inputs and nonlinearity of performance functions. The third category is the most probable point (MPP)-based methods (Hasofer and Lind 1974; Fiessler et al. 1979). The first-order reliability method (FORM) and second-order reliability methods are two popular methods in this category. The fourth category is the functional expansion-based methods. The Neumann expansion and the polynomial chaos expansion (PCE) can be classified into this group. In recent years, the PCE approach (Ghanem and Spanos 1991; Xiu and Karniadakis 2003) has been gaining more attention in uncertainty representations, stochastic mechanics, solution of stochastic differential equations, and so on. The last category is the numerical integration-based methods (Evans 1972; Seo and Kwak 2002; Lee and Kwak 2006). The statistical moments are first calculated by the direct numerical integration, and then the probability density or the tail region probability is approximated using the empirical distribution systems (Johnson et al. 1994) based on the calculated moments. For clarity, we denote the moment calculation with a full factorial set of evaluation points as a full factorial numerical integration (FFNI). A newly developed method in this category of numerical integration-based methods is the so-called dimension reduction (DR) method (Rahman and Xu 2004; Xu and Rahman 2004; Youn et al. 2006). The DR method approximates a multidimensional moment integral by multiple reduced-dimensional integrals based on additive decomposition of performance function.

When selecting a method for UP, various aspects should be considered such as the required level of uncertainty quantification, accuracy or confidence level, as well as the computational cost or efficiency. Since the performances of the above mentioned methods are affected by the problem settings such as the type of input distribution, the nonlinearity of performance function, the number of input random variables, and the required resolution, it would be beneficial to develop guidelines to choose an appropriate method that fits for a specific situation. In this paper, we present the results of our comparative study among a group of the most representative UP methods, including a few relatively recent methods, such as the univariate DR (UDR) and the PCE, as well as a few conventional approaches, such as the FFNI and the MPP-based approaches. In our studies, the results from MCS are used as a reference. Even though explicit functions are provided for our case studies, they are treated as black-box-type functions with different degrees of nonlinearity and different distribution types of input variables.

In Section 2, introductions to FFNI, UDR, and PCE are provided with emphasis on the unique aspects of each method. Test results with several problems are given in Section 3. In Section 4, a brief sum-

mary and discussions about the comparison results are provided.

2 Summary of methods

Throughout this paper, a black-box-type performance function is denoted as

$$y = g(\mathbf{X}), \tag{1}$$

where $\mathbf{X}$ is the n dimensional vector of random variables with joint probability density function (PDF) $f_{\mathbf{X}}(\mathbf{x})$ or marginal distribution functions $f_{X_i}(x_i)$ and correlations.

2.1 Full factorial numerical integration

With this approach, the statistical moments of the performance function y in (1) are calculated through the direct numerical integration using an appropriate quadrature formula. In numerical analysis, a quadrature formula is an approximation of the definite integral of a function, usually expressed as a weighted sum of function values at specified points in the domain of integration. These sampling points are often called as nodes, abscissas, integration points, or quadrature points. Once the first four moments are calculated, the complete distribution function or the probability of failure can be estimated using the empirical distribution systems (Johnson et al. 1994). Some details are provided as follows.

The m-node quadrature formula for statistical moments can be written as

$$E\left[g^k\right] = \int_{\Omega} \{g(x)\}^k f_X(x)\,\mathrm{d}x \approx \sum_{i=1}^{m} w_i \left[g(\mu + \alpha_i \sigma)\right]^k, \tag{2}$$

where α_i, w_i are the location parameter of the ith node and the corresponding weight, respectively, Ω is the domain where $f_X(x)$ is defined. The optimal locations of the nodes and the corresponding weights can be calculated using the moment-matching equations as follows:

$$\begin{aligned} M_k &= \int_{\Omega} (x-\mu)^k f_X(x)\mathrm{d}x \\ &= \sum_{i=1}^{m} w_i (\alpha_i \sigma)^k \qquad k = 0, \ldots, 2m-1, \end{aligned} \tag{3}$$

where M_k is the kth central moment of random variable X, which should be provided based on the PDF of X. This nonlinear system of equations can be solved with numerical methods to find the unique $\{\alpha_1, \cdots, \alpha_m, w_1, \cdots, w_m\}$. However, when m becomes large (e.g., >7), it is not a simple task to solve the

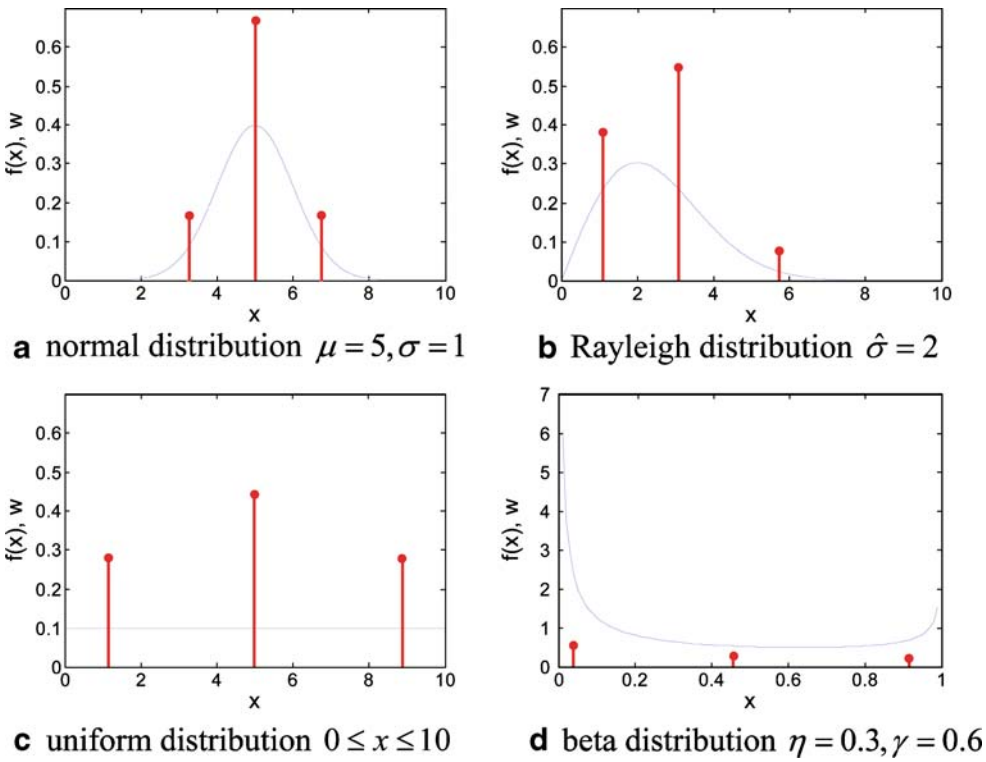

Fig. 1 **a–d** Nodes and weights in three-node quadrature formulas for four different distributions. The *vertical axis* represents the values of PDF and weights. The notations for distribution parameters are from Hahn and Shapiro (1967)

nonlinear system of equations. Figure 1 is the example of nodes and weights for some well-known distributions in three-node ($m = 3$) quadrature formulas. When X follows the normal, uniform, and exponential distribution, values of α_i and w_i can be directly derived from the Gauss–Hermite, Gauss–Legendre, and Gauss–Laguerre quadrature formula (Abramowitz and Stegun 1972), respectively, since the weighting functions of those quadrature rules have the same form with the PDF of the above three distributions. When there are n random variables in the system, the moment integral becomes an n dimensional multiple integral and can be calculated based on the tensor-product quadrature rule (Evans 1972) as follows:

$$\begin{aligned} E\left\{g^k\right\} &= \int_{\Omega_1} \cdots \int_{\Omega_n} \left[g\left(x_1, \cdots, x_n\right)\right]^k \\ &\quad \times f_{X_1,\cdots,X_n}\left(x_1, \cdots, x_n\right) \mathrm{d}x_1 \cdots \mathrm{d}x_n \\ &\cong \sum_{j_1=1}^{m} w_{j_1} \cdots \sum_{j_n=1}^{m} w_{j_n} \\ &\quad \times \left[g\left(\mu_1 + \alpha_{j_1}\sigma_1, \cdots, \mu_n + \alpha_{j_n}\sigma_n\right)\right]^k . \end{aligned} \tag{4}$$

The sampling becomes a m^n full factorial design. The integration order of this method is $(2m - 1)$, and the number of function evaluations required is m^n.

Once the four statistical moments are obtained, the probability of failure can be evaluated with the aids of the empirical distribution systems such as the Pearson system, the Johnson system, and the Gram–Charlier series (Johnson et al. 1994). Pearson system approximates the PDF $f(x)$ as a solution of the differential equation following,

$$\frac{1}{f\left(x\right)} \frac{\mathrm{d}f\left(x\right)}{\mathrm{d}x} = -\frac{\overline{x} + a}{c_0 + c_1\overline{x} + c_2\overline{x}^2}, \tag{5}$$

where $\overline{x} = x - \mu$ and, a, c_0, c_1, and c_2 are coefficients calculated from the first four central moments of random variable x whose PDF is to be approximated.

2.2 Univariate dimension reduction method

The UDR method (Rahman and Xu 2004; Xu and Rahman 2004; Youn et al. 2006) approximates a multivariate function with multiple univariate functions, which can be used for efficient calculation of multivariate statistical moment integration.

To save the computational cost, the performance function $g(\mathbf{X})$ is approximated by a sum of univariate functions, which depend on only one random variable with the other variables fixed to their mean values. If we denote these univariate functions as g_i, then the approximation can be written as:

$$\begin{aligned} g\left(\mathbf{X}\right) \approx \hat{g}\left(\mathbf{X}\right) &= \sum_{i=1}^{n} g\left(\mu_1, \cdots, X_i, \cdots, \mu_n\right) \\ &\quad - \left(n-1\right) g\left(\mu_1, \cdots, \mu_n\right) \\ &= \sum_{i=1}^{n} g_i\left(X_i\right) - \left(n-1\right) g\left(\boldsymbol{\mu}_{\mathbf{X}}\right), \end{aligned} \tag{6}$$

where μ_i denotes the mean value of ith random variable.

It can be shown that the Taylor series expansion of the univariate approximation $\hat{g}\left(\mathbf{X}\right)$ contains all single variable terms of Taylor series of $g\left(\mathbf{X}\right)$. This means that the approximation error is contributed by the terms with two or more variables in the expansion of $g\left(\mathbf{X}\right)$. Under the expectation operator, the odd powered terms in the approximation error disappear, and the most significant term in the remaining error is the fourth-order mixed derivative term $\left(x_i^2 x_j^2\right)$, which usually has a much smaller effect than the lower-order terms in the univariate approximation.

The univariate decomposition can be applied to the statistical moment integral, with the condition that the random variables should be independent with each other. When the variables are correlated, they should be transformed into independent variables with Rosenblatt transformation. The kth moment of $g\left(\mathbf{X}\right)$ is approximated as follows:

$$E\left[g^k\left(\mathbf{X}\right)\right] \approx E\left[\hat{g}^k\left(\mathbf{X}\right)\right] = E\left[\left\{\sum_{i=1}^{n} g_i\left(X_i\right) - \left(n-1\right) g\left(\boldsymbol{\mu}_{\mathbf{X}}\right)\right\}^k\right]. \tag{7}$$

These operations can be performed algebraically, and the results can be expressed in terms of moments of univariate functions, say $E\left[g_i^l\right], i = 1, \cdots, n \; l = 0, \cdots, k$. In Rahman and Xu (2004), a recursive formula for this calculation is proposed.

The moments of g_i can be calculated using the one-dimensional numerical integration based on the moment-based quadrature formula. Schemes introduced in Section 2.1 can also be used. If we use the same number of nodes m for one-dimensional integration of all the g_i, then the number of $g(\mathbf{x})$ evaluations required becomes $(m-1)\,n + 1$ at least and $mn + 1$ at most (n= number of random variables; Fig. 2). The empirical distribution system introduced in Section 2.1 needs to be applied to get the full distribution function from the moments to calculate the probability of failure.

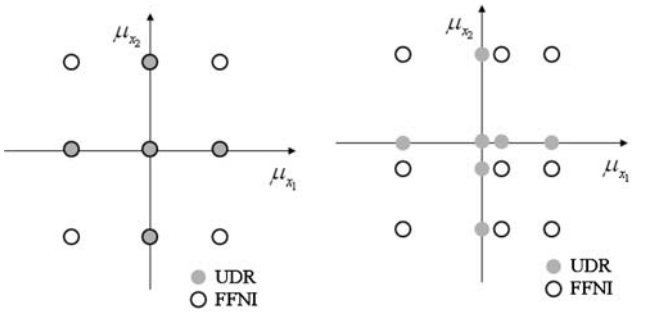

a Symmetric distribution case **b** Dissymmetric distribution case

Fig. 2 **a**, **b** Evaluation points for UDR and FFNI when three-node quadrature formula is used

2.3 Polynomial chaos expansion

The PCE method belongs to the category of functional expansion-based methods. The PCE of a square integrable random variable $u(\theta)$ can be written as (Ghanem and Spanos 1991)

$$u(\theta) = a_0\Gamma_0 + \sum_{i_1=1}^{\infty} a_{i_1}\Gamma_1\left(\xi_{i_1}(\theta)\right) + \sum_{i_1=1}^{\infty}\sum_{i_2=1}^{i_1} a_{i_1 i_2}\Gamma_2\left(\xi_{i_1}(\theta), \xi_{i_2}(\theta)\right) + \sum_{i_1=1}^{\infty}\sum_{i_2=1}^{i_1}\sum_{i_3=1}^{i_2} a_{i_1 i_2 i_3}\Gamma_3\left(\xi_{i_1}(\theta), \xi_{i_2}(\theta), \xi_{i_3}(\theta)\right) + \cdots, \tag{8}$$

where $\{\xi_i(\theta)\}_{i=1}^{\infty}$ is a set of standard normal variables, Γ_p is a generic element in the set of multidimensional Hermite polynomials of order p, and a_i are the deterministic coefficients. θ is a parameter indicating that the quantities involved are random variables defined over a space of random events. We can rewrite (8) in a simpler form as

$$u(\theta) = \sum_{i=0}^{\infty} b_i \Psi_i(\xi(\theta)), \tag{9}$$

where b_i, $\Psi_i(\xi)$ correspond to $a_{i_1\cdots i_p}$, $\Gamma_p\left(\xi_{i_1}, \cdots, \xi_{i_p}\right)$, respectively. For example, the two-dimensional PCE of second order (p =2) can be written as

$$u(\theta) = b_0 + b_1\xi_1(\theta) + b_2\xi_2(\theta) + b_3\left(\xi_1^2(\theta) - 1\right) + b_4\xi_1(\theta)\xi_2(\theta) + b_5\left(\xi_2^2(\theta) - 1\right). \tag{10}$$

Some notable properties of Hermite polynomials are

$$E\left[\Psi_i\Psi_j\right] = E\left[\Psi_i^2\right]\delta_{ij}, \tag{11}$$

$$E[\Psi_i] = 0 \quad \text{for } i \neq 0. \tag{12}$$

When there are n random inputs in the system as in (1), the output responses can be approximated by n-dimensional PCE, truncated at some order p. In this case, the number of terms in PCE becomes $P+1$ where P is given as

$$P = \sum_{s=1}^{p}\frac{1}{s!}\left\{\prod_{r=0}^{s-1}(n+r)\right\}. \tag{13}$$

Then, the PC approximation is written as

$$y \approx y^{(P)} = \sum_{i=0}^{P} b_i\Psi_i(\xi), \tag{14}$$

where ξ is a standard normal random vector of n dimension.

The coefficients in (14) can be calculated based on the orthogonality (11) of Hermite polynomials. Multiplying $\Psi_j(\xi)$ on both sides of (14) and taking the expectation, we can obtain b_j as follows:

$$b_j = E\left[y\Psi_j(\xi)\right] \Big/ E\left[\Psi_j^2(\xi)\right]. \tag{15}$$

While the denominator term in (15) can be evaluated analytically, the expectation in the numerator needs to be evaluated with sampling or numerical integration schemes. Approaches using the Latin Hyper cube sampling (Choi et al. 2004) and the numerical integration (Xiu 2007) have been reported. One issue related to the procedure is how to treat the non-normal random inputs. It is reported that the convergence rate of Hermite PCE deteriorates when the inputs are non-normal, even though the rate is significantly superior to that of crude MCS in most cases. A generalized PCE (Xiu and Karniadakis 2003) with different polynomial bases has been proposed to solve this problem with various orthogonal polynomials in the Askey scheme (Shoutens 2000). With the generalized PCE, non-normal distributions such as beta, gamma, and uniform distributions can be used as standard inputs. The selection of polynomial bases has been made more general in the work of Wan and Karniadakis (2006) who propose the chaos expansion with arbitrary probability measures.

Using different polynomial bases is one way to treat non-normal random inputs; the other way is to use transformation (Tatang 1995). The comparison between these two approaches was performed by Choi

et al. (2004). It was reported that the use of generalized PCE guarantees faster convergence, but the use of transformation is easier in implementation.

In our study, we only focus on testing the PCE with Hermite polynomial basis. The m^n FFNI with inverse Rosenblatt transformation is implemented to calculate the coefficients in (15). The detailed procedure is as follows:

1. Define transformations that map standard normal variable ξ_i to random variable X_i as

$$X_i = T_i(\xi_i) = F^{-1}(\Phi(\xi_i)) \quad i = 1, \cdots, n, \tag{16}$$

   where F denotes the cumulative distribution function (CDF) of the original random variable and Φ is the CDF of the standard normal distribution. It is assumed that the variables of X_i are independent with each other.
2. Choose nodes and weights $\{l_{i\cdot j}, w_{i\cdot j}\}$ from the Gauss–Hermite quadrature formula.
3. The coefficients b_i is calculated as

$$b_i = \left[\sum_{j_1=1}^{m} w_{j_1} \cdots \sum_{j_1=1}^{m} w_{j_n} g\left(T_1\left(l_{1\cdot j_1}\right), \cdots, T_n\left(l_{n\cdot j_n}\right)\right) \Psi_i\left(l_{1\cdot j_1}, \cdots, l_{n\cdot j_n}\right) \right] \Big/ E\left[\Psi_i^2\right], \tag{17}$$

   where the expectation in denominator can be evaluated analytically.

The result of PCE is a random variable expressed in terms of standard normal variables. This is different from other methods whose outputs are usually measures of uncertainty such as moments. The above procedure of PCE can be thought of as a construction of a non-normal random variable with projection onto the orthogonal basis of random variable space based on the observational data. Once the expansion function is obtained, the moments and probability of failure can be derived if needed.

3 Comparative studies

Four examples are tested to compare the performance of the representative methods introduced earlier. The examples are summarized in Table 1. The first example, which is one-dimensional, is chosen to compare the performance of the numerical integration scheme (Section 2.1) to the PCE method (Section 2.3) for the moment estimation under different function nonlinearities and different types of random inputs. The function nonlinearity is controlled by polynomial order k. To compare the robustness of the methods against the non-normality of inputs, two different input distributions are tried. Since the problem is one-dimensional, the UDR method is not included in the study.

The second example is a multidimensional problem chosen to compare the performances of FFNI, UDR, and PCE in moment estimation. The accuracy of the methods are compared with different input variability, which is controlled by the values of standard deviation σ. In addition to the aspects considered in example 1, we investigate the influence of interaction effects on the accuracy of the methods by testing two slightly different functions with different values of exponent a.

The third example is an overrunning clutch assembly known as the Fortini's clutch. With this example, we compare the accuracy and efficiency of the methods in moment and probability estimations with an emphasis on the robustness against non-normality of inputs. The probability estimations using the Pearson system based on four moments calculated by FFNI and UDR are compared with those from PCE and FORM.

The last example is an engine piston power loss analysis problem from which we investigate the performance of the methods in PDF estimation as well as the moment and probability calculation. This example illustrates how accurately a PDF can be estimated using the representative methods with a given number of function evaluations. Results are provided to illustrate the impact of using different orders and number of samples in PCE.

Table 1 List of examples for comparative studies

Example number	Example	Case
Example 1:	$y = x^k \quad k = 1, 2, \ldots, 7$	Case 1: $x \sim$ normal ($\mu = 1, \sigma = 0.2$) Case 2: $x \sim$ lognormal ($\mu = 1, \sigma = 0.2$)
Example 2:	$y = x_1^a x_2^a + 2x_3^4$	Case 1: $a = 2$ $x_i \sim$ lognormal $i = 1, 2, 3$ ($\mu = 1, \sigma = 0.1, 0.2, 0.3, 0.4$) Case 2: $a = 3$ $x_i \sim$ lognormal $i = 1, 2, 3$ ($\mu = 1, \sigma = 0.1, 0.2, 0.3, 0.4$)
Example 3:	Fortini's clutch	Case 1: all normal variables Case 2: 2 non-normal variables
Example 4:	Engine piston example	Two normal random variables

For all problems, three- and five-node ($m = 3$ or 5) quadrature formulas are used for FFNI and UDR to show the effect of the number of nodes on the accuracy and computational cost. With PCE, the expansions up to fourth order ($p = 4$) are tested with coefficients calculated by the procedure described in Section 2.3 with the five-node FFNI. The number of function evaluations for PCE here is the same with that of the five-node FFNI.

In the last two problems, the FORM is applied to compare the accuracy and efficiency of probability calculations with the other three methods. The HL-RF algorithm (Hasofer and Lind 1974; Rackwitz and Fiessler 1978) is used to find the MPP when applying the FORM.

It should be noted that the effect of correlations among input random variables is not covered in our comparative study.

3.1 Example 1

$$y = X^k \quad k = 1, 2, \cdots, 7. \tag{18}$$

This example is used to compare the accuracy of numerical integration and PCE against the nonlinearity of performance function in a one-dimensional case. Two cases are tested, one with an input that follows the normal distribution and the other with the lognormal distribution.

3.1.1 Case 1: $X \sim$ normal ($\mu = 1$, $\sigma = 0.2$)

In Figs. 3 and 4, the skewness and kurtosis calculation results are depicted with the ratio to the exact values obtained analytically. NI in the legend stands for numerical integration. Results of MCS with 1,000 k samples are provided for comparison. Since the input X follows a normal distribution, the Gauss–Hermite

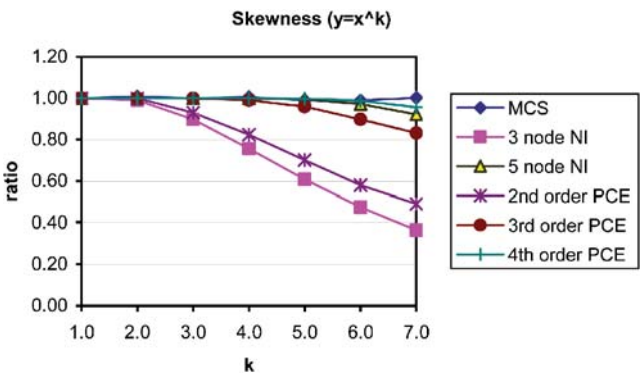

Fig. 3 Comparison of results in skewness estimation (ratio = result/exact value)

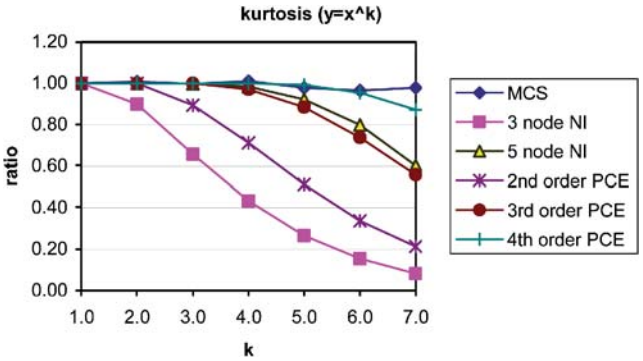

Fig. 4 Comparison of results in kurtosis estimation (ratio = result/exact value)

quadrature formula with m-node (either three or five) is used for numerical integration, and $2m-1$ integration order is expected. It means that when m is 5, the skewness results are exact up to the nonlinear order $k = 3$, and the kurtosis results are exact up to $k = 2$ since the polynomial order of the integrands for those cases ($(x^3)^3 \sim O(9)$ for skewness, $(x^2)^4 \sim O(8)$ for kurtosis) are less than or equal to the integration order of quadrature formula $2 \times 5 - 1 = 9$. It can be verified by the results obtained. The five-node numerical integration is found to be sufficient for calculating the coefficients of PCE up to fourth order in this case. PCE with coefficients obtained by numerical integration as in (17) is compared with PCE with coefficients calculated analytically (see Appendix). As the nonlinearity of y increases, the coefficients become erroneous in the higher-order terms in the PCE. The reason why higher-order expansion is still more accurate under the larger coefficient estimation error is that in this case the truncation error is more significant than the numerical error in the coefficient estimation. It is notable that for any order of expansion, $E[y^{(P)}]$ equals to $E[y]$ based on (12). Due to the orthogonality, the coefficients of low-order terms stay the same even if higher-order terms are added.

From Figs. 3 and 4, it is noted that for this example, for different orders of nonlinearity k, the accuracy follows the sequence of MCS (highest), fourth-order PCE, five-node NI, third-order PCE, second-order PCE, and the three-node NI (lowest). The fourth-order PCE shows slightly better results in skewness and kurtosis calculation than the five-node numerical integration, while both methods use the same amount of samples (5). Comparing the results of different orders of PCE, we can estimate the amount of truncation error when a lower order of PCE is used. On the other hand, the higher the order of expansion we choose, the greater the error might become in the obtained coefficients of the expansion function.

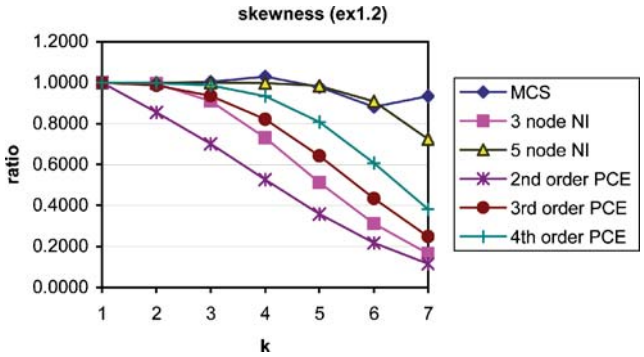

Fig. 5 Comparison of results in skewness estimation (ratio = result/exact value)

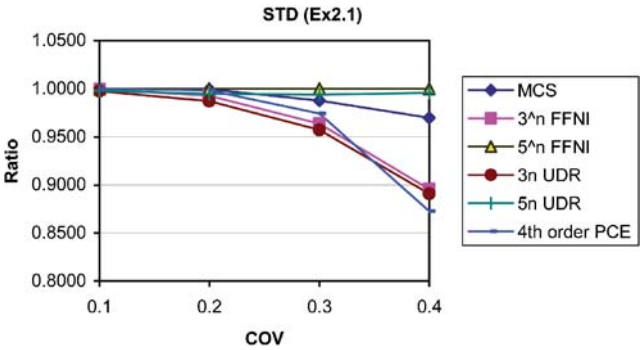

Fig. 7 Comparison of results of STD estimation (ratio = result/exact value)

3.1.2 Case 2: $X \sim$ lognormal ($\mu = 1, \sigma = 0.2$)

The same problem is tested with an input variable following the lognormal distribution. In numerical integration and MCS, no transformation is involved, but for PCE, a transformation to the standard normal variable is used during the calculation of coefficients. In this example, the analytical mapping between the normal variable and the lognormal variable is available as

$$X = \exp\left(\hat{\sigma}\xi + \hat{\mu}\right) \quad \xi \sim N\left(0, 1^2\right)$$
$$\hat{\mu} = \log \mu_X - 0.5 \log\left(\sigma_X^2 + 1\right), \quad \hat{\sigma} = \sqrt{\log\left(\sigma_X^2 + 1\right)}, \tag{19}$$

where μ_X and σ_X denote the mean and standard deviation of X, respectively.

The results of skewness and kurtosis calculation are summarized in Figs. 5 and 6. In the numerical integration, the evaluation points and weights are obtained by solving the moment-matching equation, (3). Although the results show bigger error for large k values (order of nonlinearity) compared to the results of case 1, we can see that the numerical integration with the moment matching quadrature formula provides accurate results up to $2m - 1$ polynomial order.

In case 2, the accuracy follows the sequence of MCS (highest), five-node NI, fourth-order PCE, third-order PCE, three-node NI, and second-order PCE (lowest). Contrary to the result of the normal input case, the accuracy of fourth-order PCE is worse than the five-node numerical integration, and that of the second-order PCE is worse than the three-node NI, which implies that the transformation does have a negative effect on the results. The nonlinearity of y is amplified with the transformation in (19), and the coefficient estimation becomes erroneous when the nonlinearity exceeds the integration order of the quadrature formula. This error may be reduced if we use optimal polynomial bases (Wan and Karniadakis 2006) with respect to the lognormal distribution instead of using transformation. Comparison of such alternative approaches is not within the scope of our study.

3.2 Example 2

The second example is a three-dimensional polynomial

$$y = X_1^a X_2^a + 2X_3^4, \tag{20}$$

where the variables X_i follow the lognormal distribution with mean 1. Four values of the standard deviation,

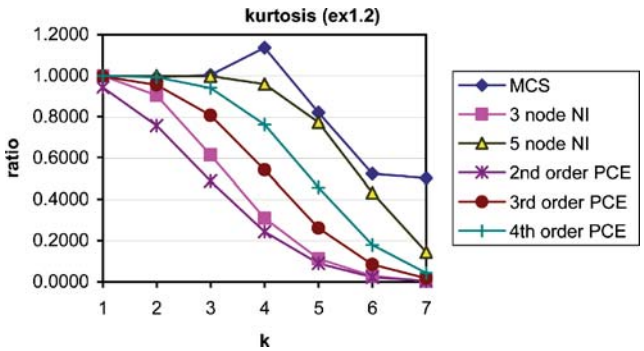

Fig. 6 Comparison of results in kurtosis estimation (ratio = result/exact value)

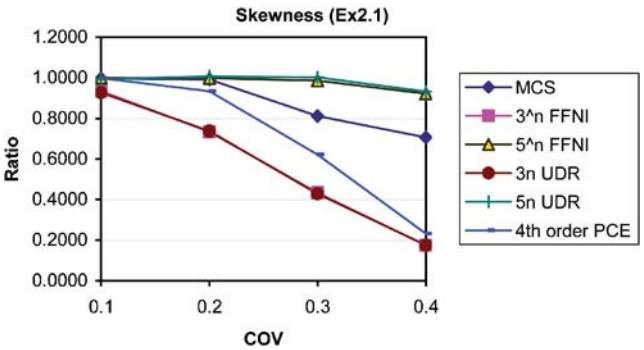

Fig. 8 Comparison of results of skewness estimation (ratio = result/exact value)

Table 2 Number of function evaluations in example 2

Method	MCS	3^n FFNI	5^n FFNI	$3n$ UDR	$5n$ UDR	Fourth PCE
Fn calls	1,000 k	27	125	7	13	125

0.1, 0.2, 0.3, and 0.4, are tested to examine the effect of variability of inputs on the moment estimation. In addition, we intend to observe the effect of interactions among variables on the performance of the methods by trying several values of a in (20). When calculating the PC coefficients, the transformation in (19) is used again.

3.2.1 Case 1: a = 2

The results of standard deviation and skewness calculations are summarized in Figs. 7 and 8. From the figures, it is seen that the results of UDR is almost identical with that from the FFNI, which implies that the univariate decomposition is valid for y; that is, the interaction effects among variables are not significant in this example. The result of PCE is much worse than that from the 5^n FFNI, which is due to the non-normality of the input random variables as in case 2 of example 1. Transformation does not always result in the degradation of accuracy; however, we can see that care must be taken when integrating a function with transformed variables. From Table 2, we note that the number of function evaluations for UDR is much less than that used for the other methods.

3.2.2 Case 2: a = 3

By increasing a, we expect that the interaction effect between X_1 and X_2 becomes more significant. The analysis results of the standard deviation and skewness are shown in Figs. 9 and 10. The computational costs are the same as in case 1 (Table 2). Compared to the results of case 1, the results of UDR show considerable discrepancies with those of FFNI and MCS especially when the standard deviations (σ) of variables are large, while FFNI still gives very close results to that of MCS. This implies that as the interaction effects grow, the error of using UDR increases.

3.3 Fortini's clutch

The third example is the Fortini's clutch (Fig. 11) used in many tolerance analysis literature (Creveling 1997). The contact angle y is given in terms of the independent component variables, X_1, X_2, X_3, and X_4 as follows:

$$y = \arccos\left(\frac{X_1 + 0.5\,(X_2 + X_3)}{X_4 - 0.5\,(X_2 + X_3)}\right). \tag{21}$$

The moments and probabilities at the left tail region of y are calculated with all methods. The Pearson system is used with FFNI and also with UDR to calculate the probability, while the probability of PCE is calculated by MCS with one million samples. To see the effect of non-normality of input variables, two different input settings are tried, one with all normally distributed variables, and the other with two non-normal variables.

3.3.1 Case 1: all normal inputs

The distribution parameters are summarized in Table 3, and the results of analysis are given in Table 4. All the methods calculate moments accurately except the UDR method. The skewness and kurtosis estimation of the $5n$ UDR is worse than that of 3^n FFNI. This means that there exist significant interaction effects between variables, and it is verified by the analysis of

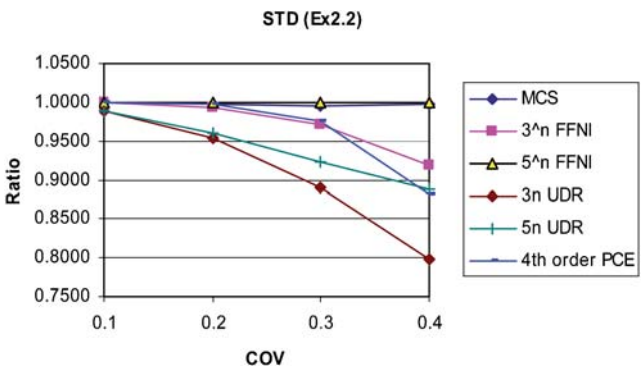

Fig. 9 Comparison of results of STD estimation (ratio = result/exact value)

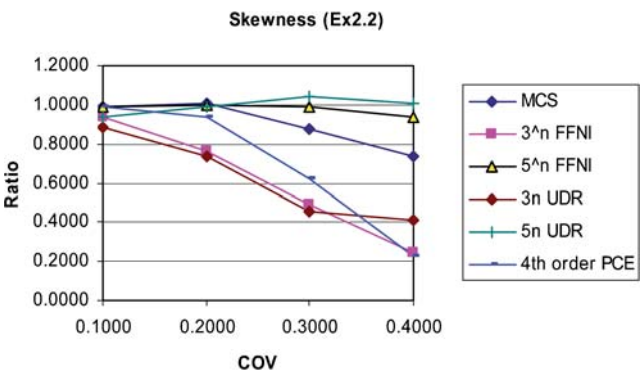

Fig. 10 Comparison of results of skewness estimation (ratio = result/exact value)

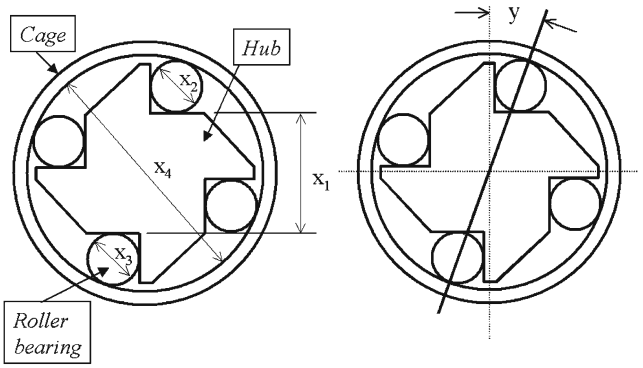

Fig. 11 Fortini's clutch

variance that the interaction between X_1 and X_4 is important. The same reason contributes to the errors in the probability estimation. It is noted that this error does not reduce much by increasing the number of nodes for one-dimensional integrations. However, the outstanding efficiency of UDR is notable. The performance of FORM is very satisfactory in both accuracy and efficiency. The limit state functions are set as ($y-$ angle), and different numbers of function evaluations are used for different limit values. For the probability values calculated by MCS, the error bounds with 95% confidence are provided in Table 4. The error bound with (1 - α)% confidence can be estimated as

$$\varepsilon = z_{1-\alpha/2}\sqrt{\frac{P(1-P)}{N}}, \tag{22}$$

where $z_{1-\alpha/2}$ denotes the $(1 - \alpha/2)$ quantile of the standard normal distribution, P is the probability value, and N is the number of samples (Law and Kelton 1982). The coefficients of PCE are calculated by 5^n FFNI, and the results are as accurate as 5^n FFNI.

3.3.2 Case 2: with 2 non-normal variables

The input X_1 is assumed to follow the beta distribution with parameters $\eta = \gamma = 5.0$, and X_4 is assumed to follow the Rayleigh distribution with the same means and standard deviations with case 1 (Table 5). The notations of distribution parameters follow those in Hahn and Shapiro (1967). Results are summarized in Table 6.

The trends are almost similar with case 1, except that the HL-RF algorithm used in FORM has some difficulties in finding the MPP when the probability is small. The divergence occurs when the search point of the HL-RF algorithm goes outside the domain where the non-normal variables are defined. FFNI shows consistently good results and similarly to the results of case 1, and UDR shows some errors in high-order moments and probability. However, we can see that the estimation of the mean and standard deviation by UDR is still good, and there is no additional loss of accuracy caused by non-normality of inputs. It can be concluded that the probability calculation based on moments becomes advantageous when non-normality of inputs are significant. The accuracy of PCE is good in this case even though the inverse Rosenblatt transformation is used for X_1 and X_4. This observation is different from the trend shown in examples 1 and 2 where the use of transformation causes considerable degradation of PCE accuracy.

3.4 Engine piston power loss analysis

The last example is from the Piston-ring/Cylinder-liner example used by Kokkolaras et al. (2006) and Liu et al. (2006). The performance of interest is the power loss due to the friction between the piston ring and the cylinder liner. Our target is to find the probability density function of power loss and also compute the probability in the tail region. The prediction model for power loss due to friction has four inputs, ring surface roughness, liner surface roughness, liner Young's modulus, and liner hardness. The first two inputs are treated as random variables following normal distributions with mean 4.0 and 6.1193 μm, respectively, and with unit variance. The other two input variables are assumed to be deterministic with values 80 GPa and 240 BHV, respectively. The analysis results are summarized in Table 7. The computational costs (number of power loss calculations) are also listed in the table.

The moment estimation results of all methods closely match with each other except the kurtosis calculated by 3^n FFNI and $3n$ UDR, which is due to the nonlinearity of the power loss function. The significance of this

Table 3 Input random variables for Fortini's clutch example (case 1)

Component	Distribution type	Mean (mm)	Standard deviation (mm)
X_1	Normal	55.29	0.0793
X_2	Normal	22.86	0.0043
X_3	Normal	22.86	0.0043
X_4	Normal	101.60	0.0793

Table 4 Uncertainty analysis results of Fortini's clutch example (case 1)

	MCS	3^n FFNI	5^n FFNI	$3n$ UDR	$5n$ UDR	Fourth PCE	FORM
Mean (rad)	0.1219	0.1219	0.1219	0.1219	0.1219	0.1219	
Standard deviation (rad)	0.0118	0.0118	0.0118	0.0117	0.0117	0.0118	
Skewness	−0.3193	−0.3082	−0.3157	−0.1436	−0.1498	−0.3190	
Kurtosis	3.2878	3.2000	3.2827	3.0000	3.0669	3.3133	
Pr($y < 4$ deg)	2.070E-04 (±2.8E-05)[a]	1.257E-04	1.732E-04	1.789E-05	3.250E-05	1.667E-04	1.810E-04
Pr($y < 5$ deg)	4.690E-03 (±1.4E-04)[a]	4.514E-03	4.830E-03	2.490E-03	2.781E-03	4.7707E-03	4.723E-03
Pr($y < 6$ deg)	7.836E-02 (±5.3E-04)[a]	7.904E-02	7.849E-02	7.482E-02	7.452E-02	7.8437E-02	7.811E-02
Fn call	1,000 k	81	625	9	17	625	(46,36,31)[b]

[a]Error bounds calculated with 95% confidence
[b]46 function evaluations for Pr($y < 4$ deg), 36 for Pr($y < 5$ deg), 31 for Pr($y < 6$ deg)

Table 5 Input random variables for Fortini's clutch example (case 2)

	Distribution	Mean (mm)	Standard deviation (mm)	Parameters for non-normal distributions
X_1	Beta	55.29	0.0793	$\gamma_1 = \eta_1 = 5.0$[a]
X_2	Normal	22.86	0.0043	–
X_3	Normal	22.86	0.0043	–
X_4	Rayleigh	101.60	0.0793	$\hat{\sigma}_4 = 0.1211$[b]

[a]$55.0269 \leq x_1 \leq 55.5531$
[b]$x_4 \geq 101.45$

Table 6 Analysis results of Fortini's clutch example (case 2)

	MCS (1,000 k)	3^n FFNI	5^n FFNI	$3n$ UDR	$5n$ UDR	Fourth PCE	FORM
Mean (rad)	0.1219	0.1219	0.1219	0.1219	0.1219	0.1219	
Standard deviation (rad)	0.0117	0.0117	0.0117	0.0116	0.0116	0.0117	
Skewness	−0.0516	−0.0497	−0.0530	0.0989	0.0964	−0.0577	
Kurtosis	2.8810	2.8488	2.8827	2.8401	2.8662	2.8930	
Pr($y < 4$ deg)	0.000E +00 (±0.0)[a]	3.791E-07	1.058E-06	0.000E+00	0.000E+00	0.000E+00	Diverge
Pr($y < 5$ deg)	1.222E–03 (±6.9E-05)[a]	1.241E-03	1.296E-03	3.707E-04	4.491E-04	1.220E-03	Diverge
Pr($y < 6$ deg)	7.381E-02 (±5.1E-04)[a]	7.288E-02	7.272E-02	6.671E-02	6.668E-02	7.402E-02	8.771E-02
Fn call	1000 k	81	625	9	17	625	31

[a]Error bounds calculated with 95% confidence

Table 7 Analysis results of engine piston example (PL: power loss)

	MCS	3^n FFNI	5^n FFNI	$3n$ UDR	$5n$ UDR	Fourth PCE	FORM
Mean	0.3931	0.3920	0.3924	0.3920	0.3926	0.3924	
Standard deviation	0.0311	0.0299	0.0300	0.0300	0.0302	0.0300	
Skewness	−0.5855	−0.5867	−0.5822	−0.5663	−0.5503	−0.58460	
Kurtosis	3.3041	3.0406	3.4336	3.1188	3.4833	3.46129	
Pr(PL < 0.3)	5.400E-03 (±4.5E-04)[a]	3.684E-03	5.161E-03	4.117E-03	5.278E-03	5.700E-03	1.903E-03
Pr(PL < 0.45)	9.970E-01 (±3.4E-04)[a]	9.996E-01	9.922E-01	9.972E-01	9.889E-01	1.000E-00	9.981E-01
Fn call	100 k	9	25	5	9	25	(15, 30)[b]

[a]Error bounds calculated with 95% confidence
[b]15 function evaluations for Pr(PL < 0.3), 30 for Pr(PL < 0.45)

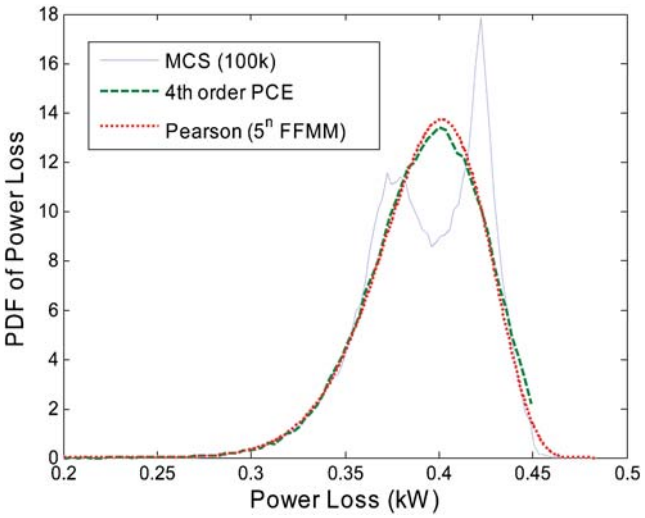

Fig. 12 PDF of power loss function

error obviously depends on the situation, our target of analysis, the confidence level required, and so on.

In probability calculation results, it is seen that 5^n FFNI, $5n$ UDR, and the fourth-order PCE match closely with the result by MCS, while 3^n FFNI and $3n$ UDR and FORM underestimate the probability at the distribution tail. It is natural that the errors in moment estimation result in errors in probability calculation. The error in the result of FORM is related to the nonlinearity of the power loss function.

In Fig. 12, the PDF of the power loss function is plotted. The PDF of the PCE is obtained by running MCS on the PCE, and the moments obtained by 5^n FFNI are used with the Pearson system to determine a PDF curve. We found that the actual PDF obtained by the MCS has an irregular shape with double peaks, but both the Pearson system based on the first four moments and the PCE fail to find the accurate shape of the PDF in this example.

The Pearson system is not capable of representing such an irregular shape, and it is an inherent limitation of fitting a PDF using a small number of moments. This example further verifies the notion that the PDF estimated by the first few moments is not unique.

The PCE can represent any square integrable random variable in theory; however, this problem shows that the convergence to the real PDF might be very slow in some cases. We further investigate PCE with a different expansion order and different number of nodes, m in (17) for coefficient calculation, to see if PCE can really represent a random variable with very irregular shape of PDF and what is the necessary computational cost to achieve that. Some results are provided in Fig. 13. It is found that to obtain a PDF close to the actual one (see Fig. 13d), for this problem, we need at least 15th-order expansion ($p \geq 15$) with

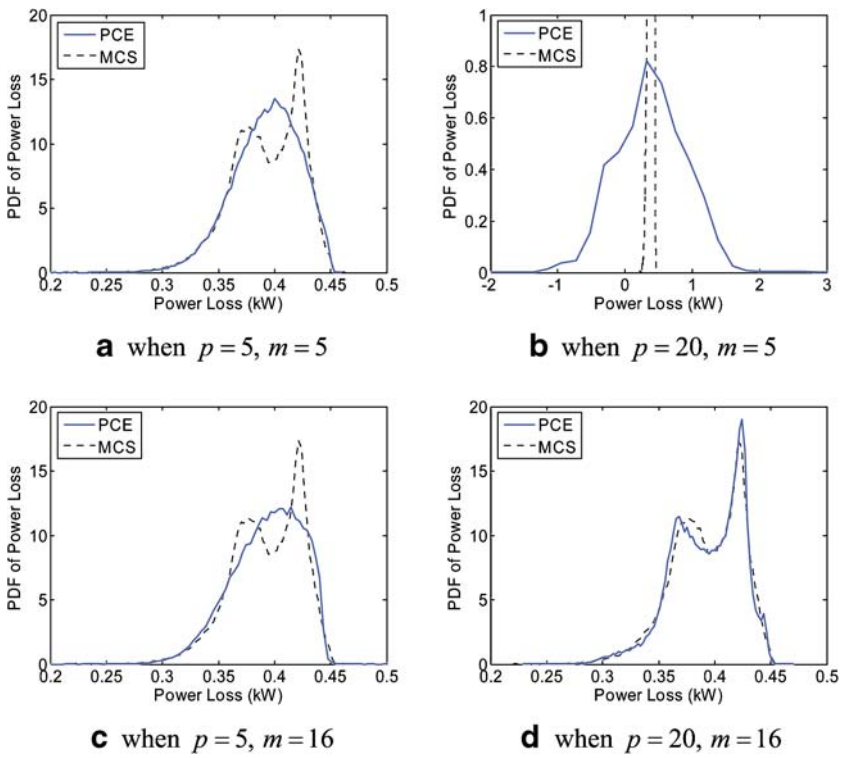

Fig. 13 **a–d** PDF estimation using PCE with different orders and number of samples

coefficients calculated by numerical integration using more than ten nodes in each dimension ($m \geq 10$), which means more than 100 nodes in total in two dimensions.

In Fig. 11, it is observed that if we increase the order of expansion but without sufficient accuracy in coefficient calculation (a to b in Fig. 13), the error in the expansion coefficients accumulates and can lead to a totally wrong solution, even divergence. On the other hand, if we increase only the number of nodes m in the coefficients calculation (a to c in Fig. 13), the truncation error of PCE still exists, and the PDF estimation does not improve much. In Fig. 13c, the computational resources are wasted since we expand only up to fifth order with data sufficient for expansions up to 20th order as in Fig. 13d.

From these studies, we can see that the order of PCE and the required number of nodes for coefficient calculation are related with each other. With limited computational resources, the order of expansion should be carefully chosen to balance the coefficient calculation error and the truncation error. To prevent the divergence as shown in Fig. 13b, the integration order of the quadrature formula used to calculate the chaos coefficients should be at least bigger than $p + 1$. This topic of selection of convergence criteria currently lacks clear guideline in literature.

It is noted that PCE can be used to estimate PDF of propagated uncertainty with an arbitrary shape, although it may become computationally expensive. None of the other existing methods are capable of determining the PDF with an arbitrary shape except the MCS.

4 Discussions and conclusions

In the paper, several categories of UP techniques, including a few techniques that are receiving growing attention, i.e., the UDR and the PCE, are examined in depth to understand the characteristics and limitations of various methods. Comparative studies are performed using illustrative examples. Ideally, the performances should be evaluated under a considerable range of system nonlinearity, various distributions of input random variables, and various dimensionality in terms of accuracy and efficiency. Hence, it might not be plausible to judge or rank the methods with just several examples. However, through this comparison study, some characteristics, advantages, and disadvantages of each method can be generalized:

- Accuracy in moment estimation: It is noted that the UDR and FFNI methods with the same number of nodes for each dimension provide almost the same accuracy if there is no significant interaction effect among variables. It is also observed that the accuracy of UDR deteriorates as the interaction effect increases and the high-order moments (skewness and kurtosis) are more vulnerable to this error than low-order moments. It is shown that this error of UDR cannot be significantly reduced by increasing the number of nodes for integration. The accuracy of PCE depends on the method adopted to calculate its coefficients. When the inputs are normal, the fourth-order PCE shows almost the same or slightly better accuracy in moment estimation than the 5^n FFNI. It is noted that in our implementation of PCE, since 5^n FFNI is used in the calculation of coefficients, the computational cost of PCE is the same with that of 5^n FFNI. For some non-normal inputs, it is shown that the accuracy of PCE may degrade considerably due to the transformation. On the contrary, FFNI and UDR show very robust performance in terms of accuracy against the non-normality of inputs. It is concluded that in the case that the uncertainty analysis is aimed for the calculation of moments, using PCE does not have a clear advantage over using FFNI or UDR.
- Accuracy of PDF and probability estimation: FFNI and UDR can be combined with the Pearson system to determine the PDF and evaluate probability. Since the accuracy of Pearson system largely depends on the accuracy of four moments provided, the accuracy of FFNI and UDR in PDF and probability calculations are determined by their accuracy of moment estimation. It is observed that the error in the moment estimation will further lead to the errors in probability calculations. Assessing tail probability using the Pearson system is shown to be comparable to the MPP based method, sometimes even better especially when the inputs are non-normal. The fourth-order PCE shows almost the same accuracy in probability calculation with that of 5^n FFNI provided that the non-normal inputs do not cause degradation of accuracy in moment estimation. It is shown that the use of Pearson system is limited to the cases when the PDF has a regular shape with one mode, while PCE is more flexible to identify PDFs of arbitrary shapes, although the computational cost of PCE may become very expensive. Further research on the error and convergence analysis appears necessary when applying the PCE to black-box-type functions.
- Efficiency of the methods: UDR shows superb performance compared to other methods. The computational cost of FFNI increases exponentially

with the number of random variables, and FFNI seems suitable only for problems with very small dimensionality because of the "curse of dimensionality." The computational cost of UDR increases linearly with the number of random variables. The efficiency of PCE depends on the method adopted to calculate the coefficients, and the computational cost should be carefully controlled considering the order of expansion.

– Usage in design under uncertainty: From the comparison, we can see that the UDR method is very effective for design scenarios involving low-order moments of system performance function like the robust design. When using UDR in design scenarios that require high-order moments such as the reliability-based design optimization, care should be taken since the high-order moment estimation of UDR is vulnerable to error caused by interaction effects. For this reason, the MPP-based UDR was developed recently and successfully applied to reliability analysis (Rahman and Wei 2006; Lee et al. 2007). FFNI can be used well with design scenarios formulated involving moments up to a high order. However, its applicability is limited by the expensive computational cost. For PCE, we could not find a strong advantage over FFNI and UDR in design scenarios only involving performance moments. However, PCE is found to be useful when the complete PDF construction is needed, either for evaluating the probabilistic design objective such as utility function or for further propagation of uncertainty in a chain type of system.

It should be noted that our tests are focused on the commonly used formula for each method but not covering all possible variations of using these methods in literature. One other aspect that was not investigated in this study is the effect of correlations among input variables on the performance of each method. All the methods except MCS need transformation of those correlated variables into uncorrelated variables. Performances of hybrid approaches that combine multiple techniques such as the UDR method with MPP (Rahman and Wei 2006; Lee et al. 2007) and response surface method with MPP are yet studied to make the current scope of comparison manageable. With the current comparative study scope, the results have provided insights into choosing the most applicable UP technique in design under uncertainty.

Acknowledgements This work was supported by the Korea Research Foundation Grant funded by the Korean Government (MOEHRD; KRF-2006-214-D00003). The grant support from National Science Foundation 0522662 is also acknowledged.

Appendix

Table 8 PCE with coefficients calculated analytically

k	Polynomial chaos expansion
1	$y^{(p)} = 1 + 0.2\xi$
2	$y^{(p)} = 1.04 + 0.4\xi + 0.04\left(\xi^2 - 1\right)$
3	$y^{(p)} = 1.12 + 0.6240\xi + 0.12\left(\xi^2 - 1\right) + 0.008\left(\xi^3 - 3\xi\right)$
4	$y^{(p)} = 1.2448 + 0.8960\xi + 0.2496\left(\xi^2 - 1\right) + 0.0320\left(\xi^3 - 3\xi\right) + 0.0016\left(\xi^4 - 6\xi^2 + 3\right)$
5	$y^{(p)} = 1.4240 + 1.2448\xi + 0.4480\left(\xi^2 - 1\right) + 0.0832\left(\xi^3 - 3\xi\right) + 0.0080\left(\xi^4 - 6\xi^2 + 3\right)$
6	$y^{(p)} = 1.6730 + 1.7088\xi + 0.7469\left(\xi^2 - 1\right) + 0.1792\left(\xi^3 - 3z\right) + 0.0250\left(\xi^4 - 6\xi^2 + 3\right)$
7	$y^{(p)} = 2.0147 + 2.3421\xi + 1.3348\left(\xi^2 - 1\right) + 0.3485\left(\xi^3 - 3\xi\right) + 0.0672\left(\xi^4 - 6\xi^2 + 3\right)$

Table 9 PCE with coefficients calculated numerically

k	Polynomial chaos expansion
1	$y^{(p)} = 1 + 0.2\xi$
2	$y^{(p)} = 1.04 + 0.4\xi + 0.04\left(\xi^2 - 1\right)$
3	$y^{(p)} = 1.12 + 0.6240\xi + 0.12\left(\xi^2 - 1\right) + 0.008\left(\xi^3 - 3\xi\right)$
4	$y^{(p)} = 1.2448 + 0.8960\xi + 0.2496\left(\xi^2 - 1\right) + 0.0320\left(\xi^3 - 3\xi\right) + 0.0016\left(\xi^4 - 6\xi^2 + 3\right)$
5	$y^{(p)} = 1.4240 + 1.2448\xi + 0.4480\left(\xi^2 - 1\right) + 0.0832\left(\xi^3 - 3\xi\right) + 0.0080\left(\xi^4 - 6\xi^2 + 3\right)$
6	$y^{(p)} = 1.6730 + 1.7088\xi + 0.7469\left(\xi^2 - 1\right) + 0.1792\left(\xi^3 - 3\xi\right) + 0.0246\left(\xi^4 - 6\xi^2 + 3\right)$
7	$y^{(p)} = 2.0147 + 2.3421\xi + 1.1962\left(\xi^2 - 1\right) + 0.3483\left(\xi^3 - 3\xi\right) + 0.0604\left(\xi^4 - 6\xi^2 + 3\right)$

References

Abramowitz M, Stegun IA (1972) Handbook of mathematical functions (10th edn.). Dover, New York

Bucher CG (1988) Adaptive sampling—an iterative fast Monte Carlo procedure. Struct Saf 5:119–126

Choi SK, Grandhi RV, Canfield RA (2004) Structural reliability under non-Gaussian stochastic behavior. Comput Struct 82:1113–1121

Christensen P, Baker MJ (1982) Structural reliability theory and its applications. Springer, New York

Creveling CM (1997) Tolerance design: a handbook for developing optimal specifications. Addison-Wesley, Reading, MA

D'Errico JR, Zaino NA (1988) Statistical tolerancing using a modification of Taguchi's method. Technometrics 30: 397–405

Du X, Chen W (2000) Towards a better understanding of modeling feasibility robustness in engineering design. J Mech Des 122:385–394

Du X, Sudjianto A, Chen W (2004) An integrated framework for optimization under uncertainty using inverse reliability strategy. J Mech Des 126:562–570

Engelund S, Rackwitz R (1993) A benchmark study on importance sampling techniques in structural reliability. Struct Saf 12:255–276

Evans DH (1972) An application of numerical integration techniques to statistical tolerancing, III: general distributions. Technometrics 14:23–35

Fiessler B, Rackwitz R, Neumann H (1979) Quadratic limit states in structural reliability. J Eng Mech 105:661–676

Ghanem RG, Spanos PD (1991) Stochastic finite elements: a spectral approach. Springer, New York

Hasofer AM, Lind NC (1974) Exact and invariant second order code format. J Eng Mech 100(NEM1):111–121

Hahn GJ, Shapiro SS (1967) Statistical models in engineering. Wiley, New York

Hazelrigg GA (1998) A framework for decision-based engineering design. J Mech Des 120:653–658

Johnson NL, Kotz S, Balakrishnan N (1994) Continuous univariate distributions (vol 1). Wiley, New York

Kiureghian AD (1996) Structural reliability methods for seismic safety assessment: a review. Eng Struct 18:412–424

Kokkolaras M, Mourelatos ZP, Papalambros PY (2006) Design optimization of hierarchically decomposed multilevel system under uncertainty. J Mech Des 128:503–508

Law AM, Kelton WD (1982) Simulation modeling ands analysis. McGraw-Hill, New York

Lee TW, Kwak BM (1987–88) A reliability-based optimal design using advanced first order second moment method. Mech Struct Mach 15:523–542

Lee SH, Kwak BM (2006) Response surface augmented moment method for efficient reliability analysis. Struct Saf 28: 261–272

Lee I, Choi KK, Du L (2007) A new inverse reliability analysis method using MPP-based dimension reduction method (DRM). In: Proceedings of ASME 2007 international design engineering technical conference and computers and information in engineering conference (IDETC/CIE2007), Las Vegas, NV, USA

Liu W, Belytschko T, Mani A (1986) Random field finite elements. Int J Numer Methods Eng 23:1831–1845

Liu H, Chen W, Kokkolaras M, Papalambros PY, Kim HM (2006) Probabilistic analytical target cascading: a moment matching formulation for multilevel optimization under uncertainty. J Mech Des 128:991–1000

Madsen HO, Krenk S, Lind NC (2006) Methods of structural safety. Dover, Mineola, NY

McAllister CD, Simpson TW (2003) Multidisciplinary robust design optimization of an internal combustion engine. J Mech Des 125:124–130

Melchers RE (1989) Importance sampling in structural systems. Struct Saf 6:3–10

Rackwitz R, Fiessler B (1978) Structural reliability under combined random load sequences. Comput Struct 9:489–494

Rahman S, Wei D (2006) A univariate approximation at most probable point for higher-order reliability analysis. Int J Solids Struct 43:2820–2839

Rahman S, Xu H (2004) A univariate dimension-reduction method for multi-dimensional integration in stochastic mechanics. Probab Eng Mech 19:393–408

Seo HS, Kwak BM (2002) Efficient statistical tolerance analysis for general distributions using three-point information. Int J Prod Res 40:931–944

Shoutens W (2000) Stochastic processes and orthogonal polynomials. Springer, New York

Taguchi G (1978) Performance analysis design. Int J Prod Res 16:521–530

Tatang MA (1995) Direct incorporation of uncertainty in chemical and environmental engineering systems. Ph.D. thesis, MIT

Wan X, Karniadakis GE (2006) Multi-element generalized polynomial chaos for arbitrary probability measure. SIAM J Sci Comput 28:901–928

Wu YT (1994) Computational methods for efficient structural reliability and reliability sensitivity analysis. AIAA J 32: 1717–1723

Xiu D (2007) Efficient collocatioal approach for parametric uncertainty analysis. Commun Comput Phys 2:293–309

Xiu D, Karniadakis GE (2003) Modeling uncertainty in flow simulations via generalized polynomial chaos. J Comput Phis 187:137–167

Xu H, Rahman S (2004) A generalized dimension-reduction method for multi-dimensional integration in stochastic mechanics. Int J Numer Methods Eng 61:1992–2019

Youn BD, Choi KK, Park YH (2003) Hybrid analysis method for reliability-based design optimization. J Mech Des 125: 221–232

Youn BD, Xi Z, Wells LJ, Wang P (2006) Enhanced dimension reduction (eDR) method for sensitivity-free uncertainty quantification. In: Proceedings of 11th AIAA/ISSMO multidisciplinary analysis and optimization conference, Portsmouth, VA, USA